AN EXPERIMENTAL INVESTIGATION OF DISLOCATION GLIDE IN OLIVINE

By

BRENDA J. BLAKE

S.B., Massachusetts Institute of Technology

1975

SUBMITTED IN PARTIAL FULFILLMENT

OF THE REQUIREMENTS FOR THE

DEGREE OF MASTER OF

SCIENCE

at the

MASSACHUSETTS INSTITUTE OF

TECHNOLOGY

June, 1976

Signature of Author.....
Department of Earth and Planetary Sciences,
June, 1976

Certified by.....
Thesis Supervisor

Accepted by.....
Chairman, Departmental Committee on Graduate Students

ABSTRACT

An Experimental Investigation of

Dislocation Glide in Olivine

by

Brenda J. Blake

Submitted to the Department of Earth and Planetary Sciences on June, 1976, in partial fulfillment of the requirements for the degree of Master of Science.

Selectively oriented single crystals of olivine have been deformed at high temperature (1080° to 1575° C) by stress pulses of known duration to obtain estimates of glide velocities. Creep data were computed from experimental glide velocity results and dislocation densities. The stresses were corrected to a constant strain rate of 10^{-5} 1/second for both [101] and [110] orientations. Results were compared with climb limited creep data from previous work. Analysis of the experimental data revealed that the strain rate of [101] and [110] oriented single crystals of olivine is probably glide limited.

Thesis Supervisor: Christopher Goetze
Title: Assistant Professor of Geophysics

ACKNOWLEDGEMENTS

I would like to thank Prof. C. Goetze for his constant help and guidance throughout this thesis. Without his persistent nudging, these results may have never come to pass.

I would also like to thank many of my close friends at M.I.T. for unrelenting moral support in my endeavor to finish this paper. In particular, I would like to thank N. Chinn, S. Miller, and W. Short for services rendered beyond the call of duty.

TABLE OF CONTENTS

LIST OF FIGURES

LIST OF TABLES

INTRODUCTION

Olivine has been subject to extensive high temperature deformation experiments in the past decade. It is chemically and structurally stable over a wide range of pressures and temperatures. If the nature of the crystal defects and their motion can be understood then this information can be used to describe conditions in the mantle.

In a series of single crystal creep studies (Goetze and Kohlstedt, 1973, Kohlstedt and Goetze, 1974, Durham, 1975), have been interpreted as climb limited creep as proposed by Weertman, 1968.

In Weertman's model glide is rapid and does not limit the motion of dislocations. There were no data on glide velocities in olivine at that time and this could therefore not be checked. Canon and Sherby (1973) and Argon and Takeuchi (1976), and Alexander and Haasen (1968) have shown that similar behavior can result from a glide limited motion and that a stress exponent, n, of 3-3.6 in the creep law may ,in fact, be an indicator that creep is glide limited. The exponent for olivine, (Durham, 1975), is 3.6. To test this possibility a number of single crystal olivine specimens were deformed by stress pulses of known duration to obtain an estimate of glide velocities in olivine.

EXPERIMENTAL TECHNIQUE

Starting Material

The samples were cut from two crystals of San Carlos peridot. The crystals were $(Mg,Fe)_2SiO_4$ (Fo 92) and were approximately 1½ cm in diameter. The olivine lattice is orthorhombic with unit cell dimensions of 4.8Å, 10.2Å, and 6.0Å. Their respective directions are [100], [010], and [001]. The solidus and liquidus temperatures are ~1770°C and ~1870°C respectively. The total dislocation density of the starting material was $10^{4.5}$ to $10^{6.5}$ cm^{-2}.

Sample Preparation

The crystals were cut in beams with an average length of 3.4 mm, a width of 1 mm, and a varying thickness of .66, .55, or .90 mm (Table 1), with a Laser Technology Model 2005-C wire saw. These beams were crack and inclusion free. The super copper alloy wire was .008" or .02 cm. The cut wasted less than .025 cm of sample. Once an orientation was determined, many samples could be cut from a single crystal.

The orientation was determined by cutting a slice from the crystal and using a U-staged equipped optical microscope. Two orientations were used in the experiments. Ten samples had the c axis in the plane perpendicular to σ_1, while a and b were at 45° to σ_1 along the length axis (Fig. 1). Sixteen samples had the b axis in the plane perpendicular to σ_1, while a and c were 45° to σ_1. The a-b orientations had a ± 5° error determined by the optical

TABLE 1

Specimen dimensions and load applied

Specimen	Length (mm)	Width (mm)	Thickness (mm)	Load applied (gms)
7510-1B	3.3	1.01	.635	3017
7510-2B	3.2	1.01	.660	1519
7510-3B	3.4	.8	.57	1069
7510-4B	3.4	.95	.66	3000
7510-5B	3.3	.9	.29	469
7510-6B	3.2	.9	.66	589
7510-7B	3.15	.9	.29	469
7510-8B	3.2	.9	.66	2941
7510-9B	3.2	.8	.66	1110
7510-10B	3.4	.8	.66	1569
7511-1A	3.3	1.0	.55	1469
7511-2A	3.3	1.0	.55	876
7511-3A	3.35	.95	.55	869
7511-4A	3.4	.85	.55	1489
7511-5A	3.3	.9	.55	64
7511-6A	3.3	.9	.55	1025
7511-7A	3.3	.7	.55	1226
7511-8A	3.3	.9	.55	1369
7511-9A	3.4	.75	.42	438
7511-10A	3.45	.75	.9	3860
7511-11A	3.45	.85	.9	2202

TABLE 1 (cont.)

Specimen	Length (mm)	Width (mm)	Thickness (mm)	Load applied (gms)
7511-12A	3.4	.9	.9	4663
7511-13A	3.3	.95	.9	2485
7511-14A	3.2	.8	.95	691
7511-15A	3.3	.8	.95	4605
7511-16A	3.5	.75	.9	3875

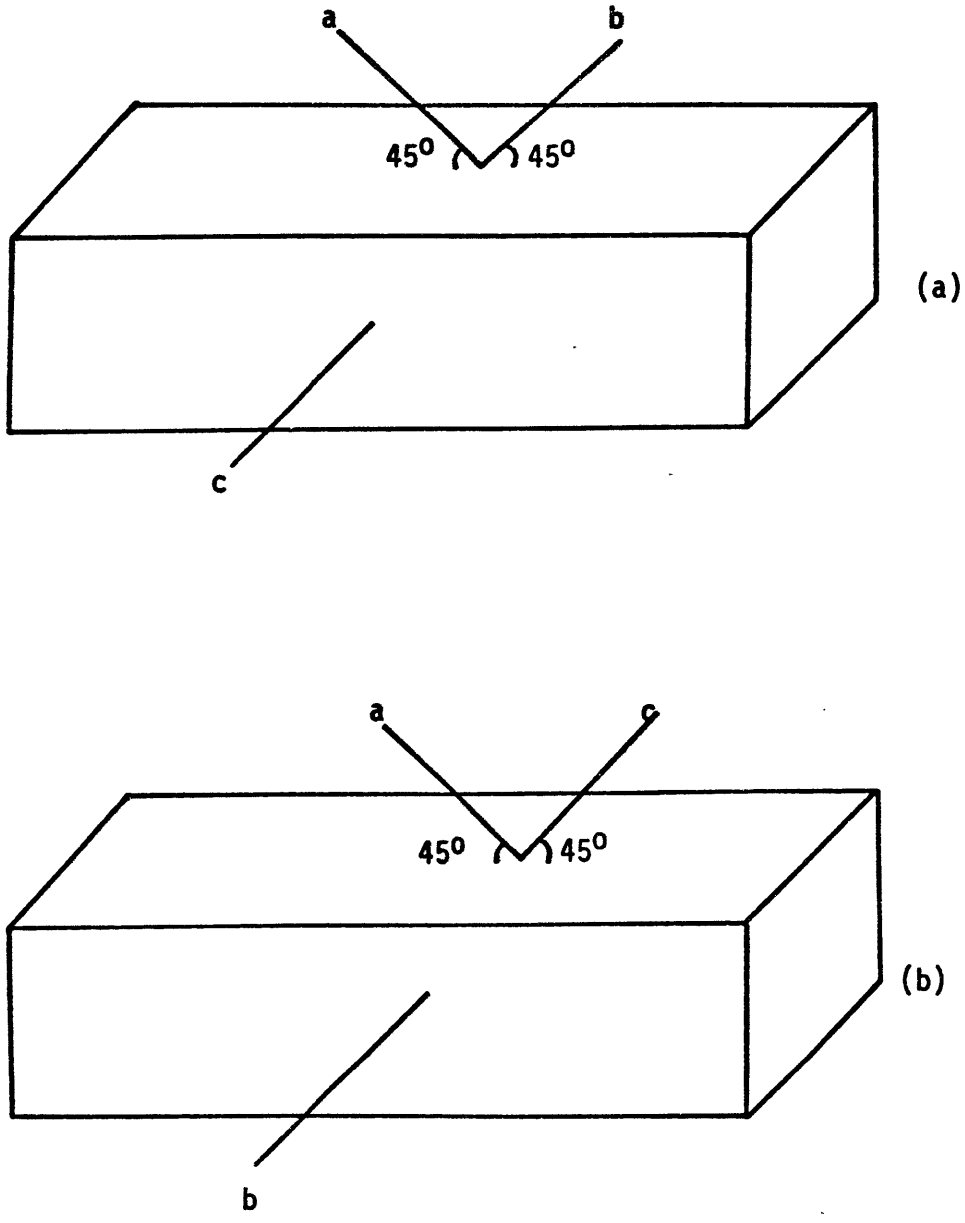

Fig. 1 Ideal orientations of a-b and a-c crystals

microscope. An error occured in the orientation of the a-c samples. Their actual orientation is shown in figure 9. The samples were polished with Al_2O_3 (1μ) powder on the top and bottom surfaces to minimize friction and seizing at the platen interfaces. Later in the series of runs, the sides were polished also.

Prior to deformation all dimensions of the sample were measured with a hand lens micrometer.

The Apparatus

Runs 7510-1B through 7510-10B and 7511-1A through 7511-16A were deformed with a dead weight load apparatus described by Durham (1975), (Fig. 2).

Molybdenum rods supported the load inside the furnace. The sample was set in a cylinder of molybdenum on a circular shelf. Another piece of molybdenum was machined to a cone shape and was set inside the cylinder (Fig. 3). This configuration gave a three point bending load. The length of the sample was not too critical. It had to be sufficiently long to set on the shelf on all four corners. The stressed length of all specimens was 2.7 mm compared to an average total length of 3.4 mm.

The fugacity of oxygen was controlled by flowing 30% CO_2-70% H_2 gas mixture through the furnace. The sample remained within the stability field of Fo 92 (Nitsan, 1974) at the temperatures used in our experiments. The samples were considered "dry olivine" since temperatures of $\sim$1000^{o}C and pressure of 1 atm for a few minutes drove off any detectable water (Goetze and Kohlstedt, 1973).

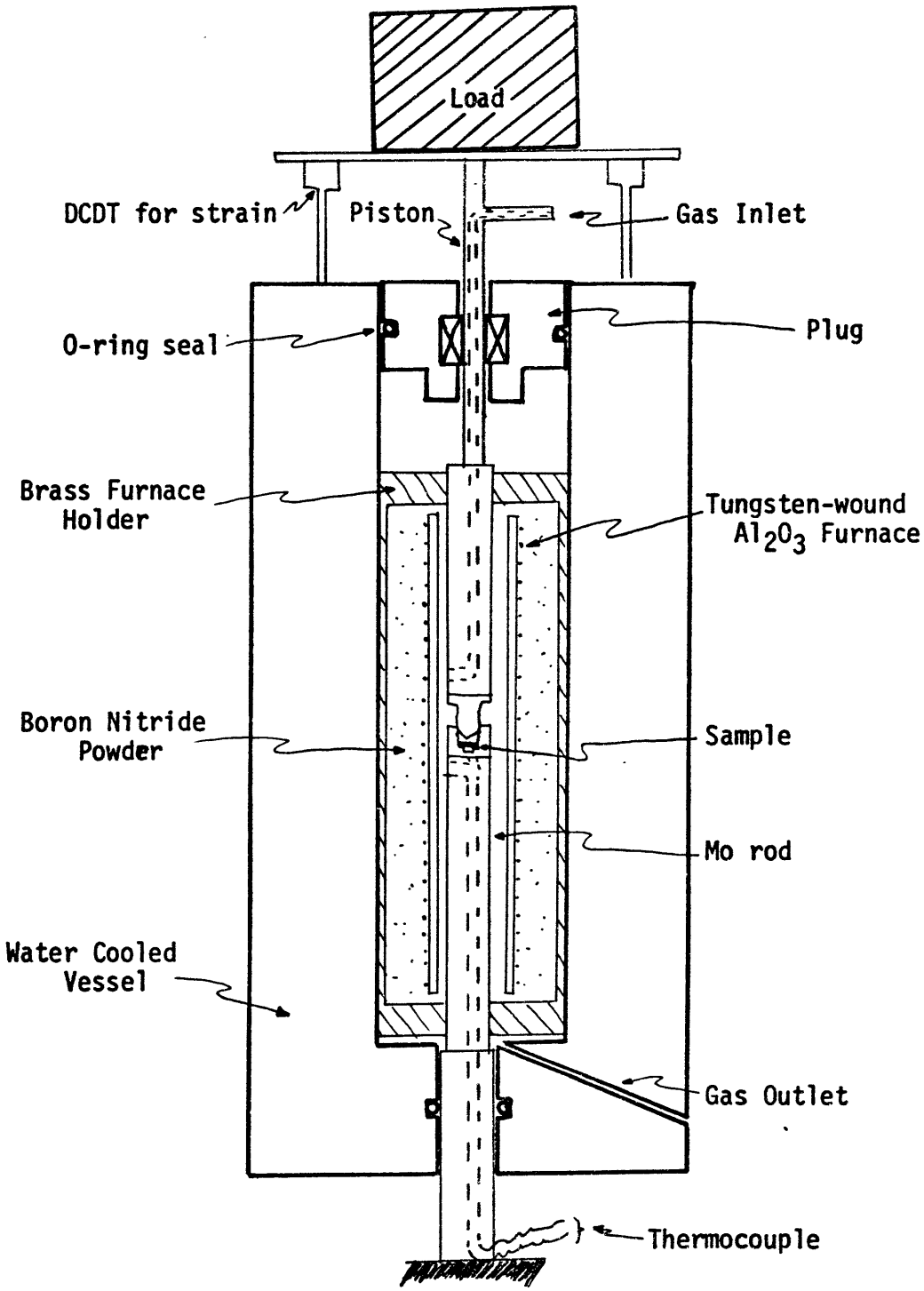

Fig. 2 Experimental Apparatus

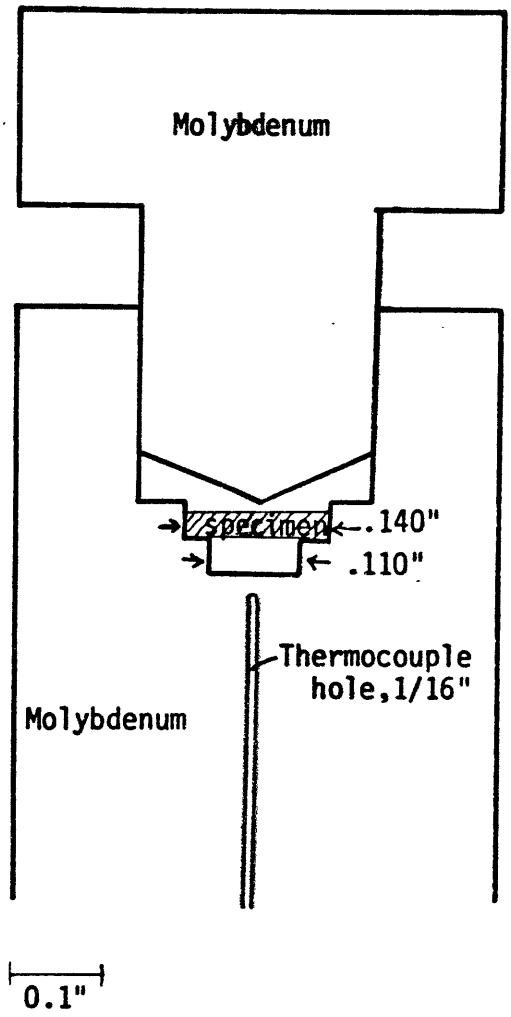

Fig. 3 Specimen holder for dry olivine single crystal beams

The temperature was measured by a W-5%, Re/W-26% thermocouple. The thermocouple sat .3 cm below the specimen. Temperatures were recorded on a chart recorder. An automatic controller maintained the desired temperature during the run to within $\pm 4^{0}$ C. The temperature was increased at a rate of $3\text{-}4^{0}$ per second.

Displacement in the sample was measured by a pair of direct current differential transformers (DCDT), mounted on the piston on top of the apparatus. Any displacements larger than a net motion of .5 mm usually meant the sample was broken. In several runs the DCDT's were not connected to allow either a very small σ to be applied, or the time that the load was applied was so short that the DCDT's could not be zeroed. In our runs the DCDT's were used to determine how the sample was reacting to the loads. With simple beam theory one can determine the stress patterns of the samples without the use of the DCDT's.

EXPERIMENTAL PROCEDURES

All runs started with an initial weight of 469 grams. This was the total weight of the molybdenum parts and the piston configuration with the DCDT's on top.

At the conclusion of the run, the furnace was turned off and the weights removed. In some instances, the rapidity of cooling down and removal of weights may have caused the samples to fracture at their bending points.

Each specimen, upon removal from the deformation furnace, was decorated in an open air horizontal furnace. The samples had been

polished with a 1.0μ Al_2O_3 grit before the run. They were placed in an Al_2O_3 alundum boat in the furnace at 920° C ± 20° C. The average length of time for an a-b orientation was 60 minutes. For a-c orientation, the time was about 1½ hours. The larger range of differential stress was exposed on the crystal sides (Fig. 4) and so the sides were the interesting sections of the crystal. The (010) side took much longer and higher temperatures to achieve the same decoration effect as the (001). A film was often left on the polished faces after decoration. This was removed by a few quick polishes with the 1.0μ Al_2O_3 grit.

Stress

The position of each dislocation was determined by taking a picture of the sample and blowing it up about sixty times. The photos were used as maps to find the location of dislocations that were to be measured. The stress on the sample was determined by using simple beam theory (Eq. 1, Fig. 4).

$$\sigma_{max} = \frac{3}{2} \frac{P_o\, g\, L}{w\, H^2} \left[1 - \frac{2H}{\pi L}\right] \qquad \text{(Timoschiko and Goodier)}$$

Eq. 1

where w = width
L = length of test section
H = thickness
P_o = load in grams
g = 980 cm/sec^2.

A plastic overlay of these curves was put on top of each picture, and the stress for that dislocation was chosen from the grid position.

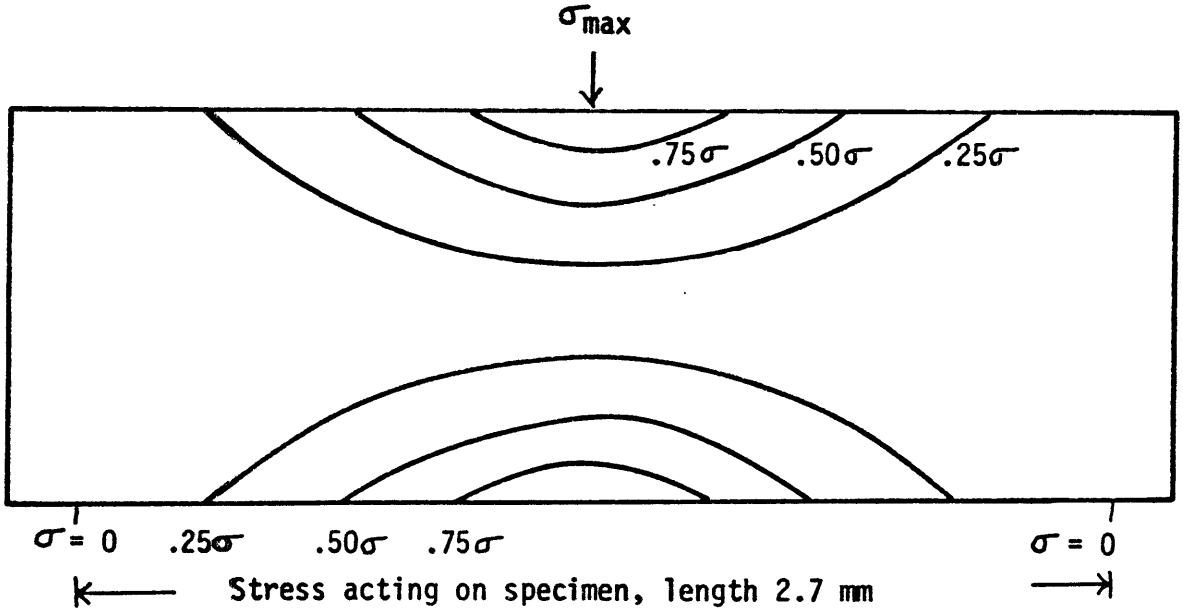

Fig. 4 Equal lines of stress in a bending beam

Amount and Velocity of Glide

The crux of this technique for measuring glide velocities was that the existing dislocation structure before the run tended to consist of gently curved and non-crystallographic dislocation line directions while the freshly formed glide loops tended to be sharply rectilinear and crystallographic. Fig. 5 shows the starting material, fig. 6 shows a region of starting material containing a few fresh dislocation loops, while fig. 7 shows a later stage in which the field is filled with many loops of the same kind. Fig. 8 shows the formation of fresh glide loops in an a-c oriented sample. The glide distance was taken to be 20μ in fig. 6, a number which is representative of the glide loop dimensions. Fig. 5 and 7 were not considered suitable for measuring the glide distance.

The glide velocity was taken to be this glide distance divided by the time that the load was applied (Johnston and Gilman, 1959).

Some of our specimens (7510-9B, 7510-10B, 7511-6A, 7511-7A) were indented or scratched on the surface with a diamond tool. Similar experiments (Gilman and Johnston; Chaudhuri, Patel, and Rubin, 1962, Prekel and Conrad; Singh and Coble, 1974) measured velocities. These induced scratches would create b = [001]. In our case the indentor created a good deal of spalling and the diamond scratch was not a fine line. The amount of deterioration on the sample was too great to measure the velocities on any potential dislocations radiating from such indents. The 7510-10B and 7511-7A samples were weakened by the indents and broke during the experiment.

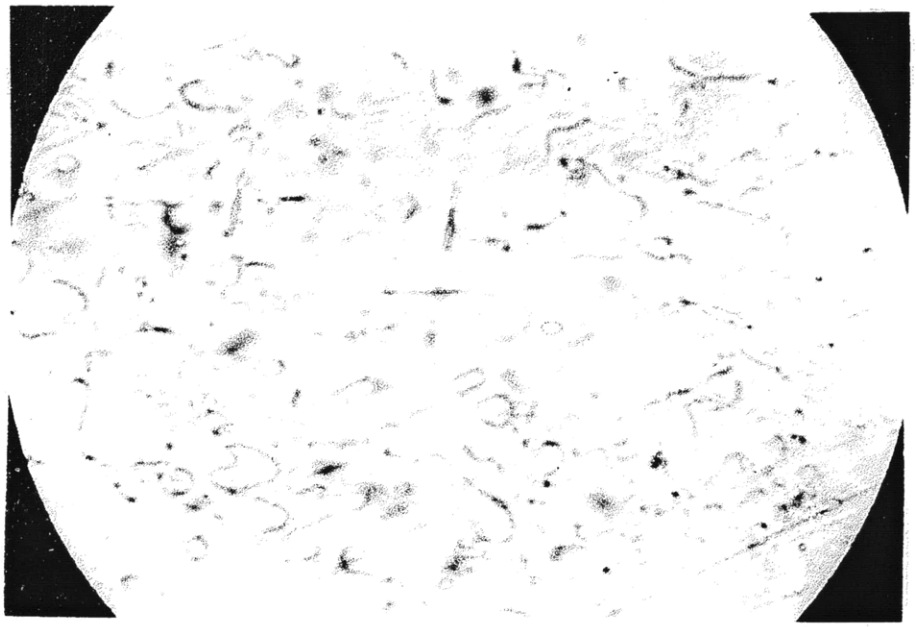

Fig. 5 Starting material, field of view 110 μ
a-b orientation

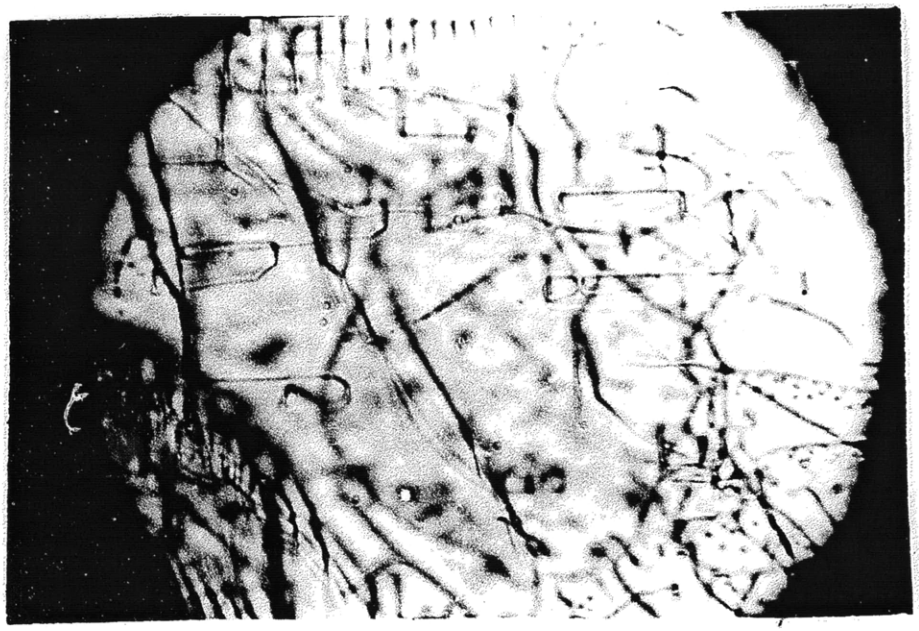

Fig. 6 Starting material with some dislocations, field of view 110 μ
a-b orientation

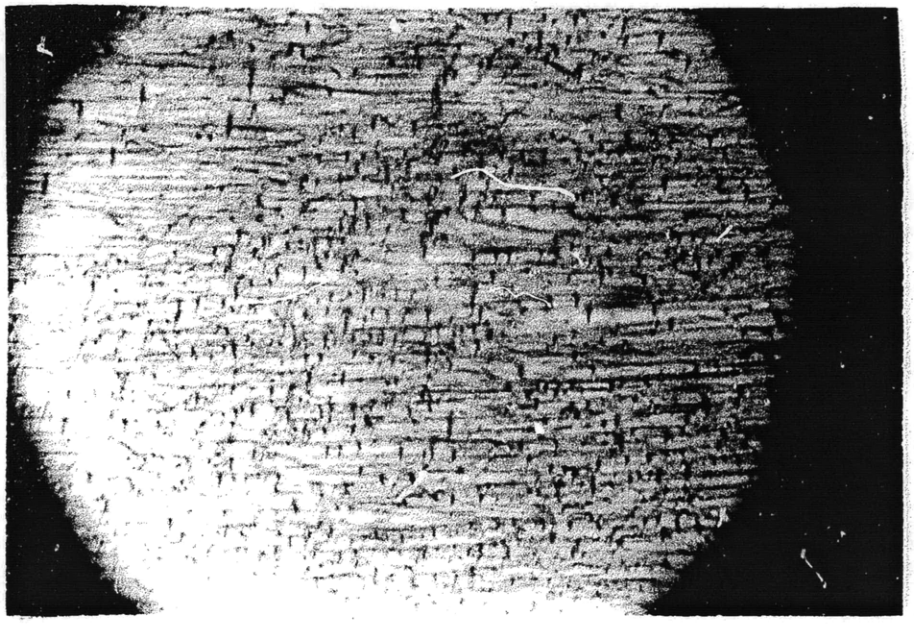

Fig. 7 Glide loops in a-b orientation, field of view 110μ

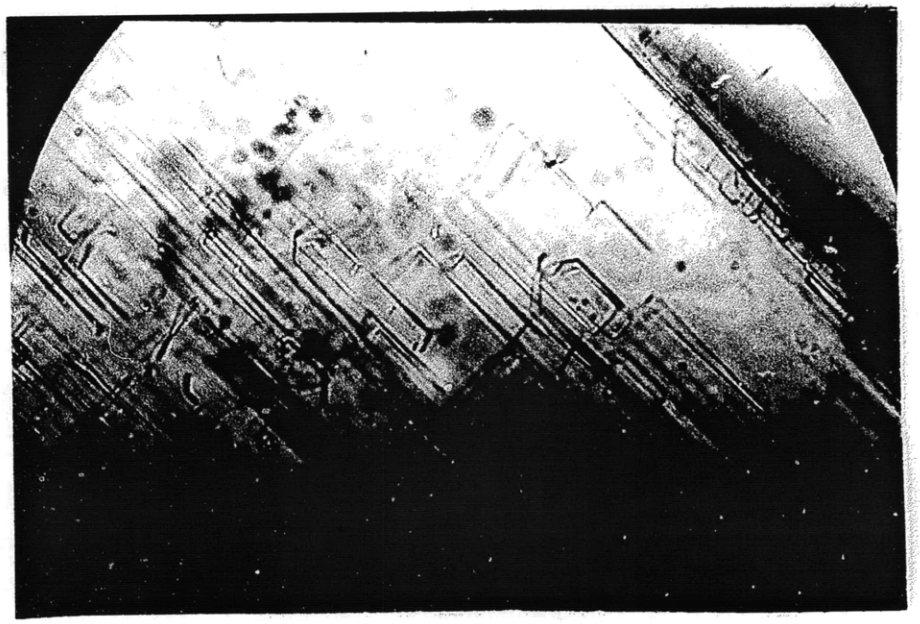

Fig. 8 Glide loops in a-c orientation, field of view 110μ

RESULTS AND DISCUSSION

The samples were oriented so that a non-zero resolved shear stress existed on as few systems as possible. A zero resolved shear stress exists on some but not all the slip systems only when one and only one of the crystallographic axes lies perpendicular to σ_1.

The samples 7510-1B through 7510-10B were oriented with a-b axes at 45° to the stress in the vertical plane and c is at 90° in the horizontal plane (Fig. 1a). Samples 7511-1A through 7511-16A were oriented with b approximately perpendicular to σ_1.

In olivine only three Burgers vectors have been identified: b = [100], [010], and [001]. Raleigh (1968), Phakey et al. (1972), Durham (1975), and Goetze and Kohlstedt (1973) have listed several techniques used in determining slip systems. Table 2 list the Burgers vectors and the active slip planes. Specimens of the a-b orientations were compatible with the slip system (010)[100]. This was expected as the a-b orientation has a large field in which the (010)[100] slip system is active (Fig. 9). The glide plane was observed in the optical microscope to be (010) and of the two possible Burgers vectors in this plane, [100] and [001], [001] experienced nominally zero resolved shear stress.

The b = [100] edges were more heavily decorated in the plane strain section. In the glide plane section the [100] screws were more visible. Most of the b = [100] edges formed straight long segments parallel to the glide plane. The [100] screws were bowed out rather than straight lines.

For the a-c orientations, the b axis had no shear stress. This orientation was used because it gave a high shear stress in the direction of [100] and [001] which are the shortest axes of the unit cell and the

TABLE 2

Olivine slip systems

slip planes	slip direction (Burgers vectors)
(010)	[100]
(001)	
(0kℓ)	
(100)	[010]
(001)	
(100)	[001]
(010)	

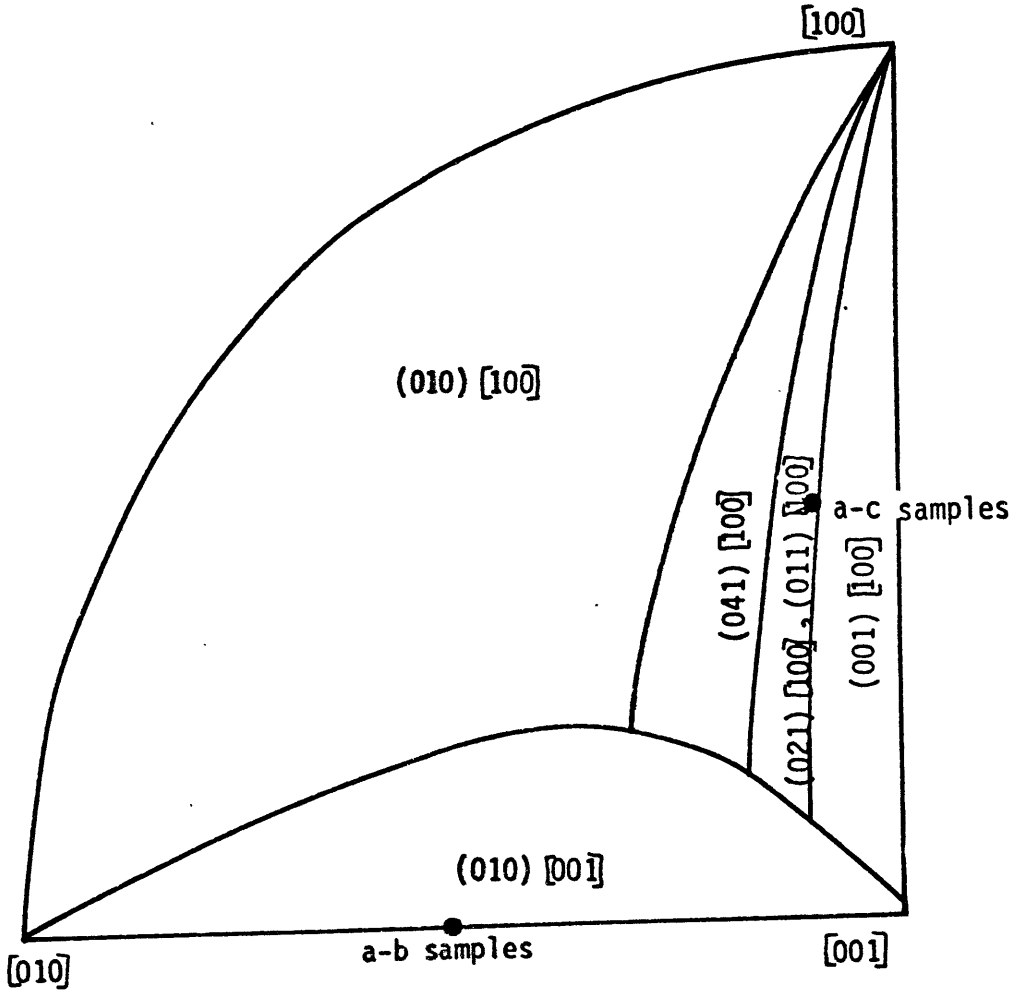
[100]
(010) [10$\bar{0}$]
(041) [10$\bar{0}$]
(021) [10$\bar{0}$]
(011) [10$\bar{0}$]
(001) [10$\bar{0}$]
a-c samples
(010) [00$\bar{1}$]
[010]
a-b samples
[001]

Fig. 9

commonest slip vectors (Phakey et al, 1972). The a-c axes were not exactly 45° from σ_1 (Fig. 9). Since our orientation was not exact, the [100] burgers had a maximum resolved shear stress on an (0kℓ) plane. At temperatures below 900° C, the Burgers vector [001] predominates over slip in other directions in the crystal (Phakey et al, 1972, Raleigh, 1968). Above 1000° C the b = [100] takes over. For high temperatures and low strain rates the slip planes in the specimens have various orientations in the zone of [100] , yielding a slip aystem of (0kℓ)[100] . This has been termed pencil glide, (Raleigh, 1968). In the microscope we observed many straight ℓ = [100] dislocation segments connected by segments lying on a variety of planes, suggestive of this pencil glide mechanism. This is also expected from Durham's plot, Fig. 9.

For a-c orientation, many dislocation segments exhibited a bubble train bringing up the tail of the glide segment(Fig.10), of the form sketched in Fig. 10a. This suggests that in these cases the steps are emitting sessile loops as they travel and are therefore not moving conservatively. This is not compatible with b = [100] but is compatible with b = [001] , the other Burgers vector found to contribute significantly to the $\dot{\epsilon}$ for specimens of this orientation (Durham, 1975). The operating Burgers vector in the a-c samples is therefore not known.

For T approaching 1600° C, slip involving b = [100] is preferred at most orientations of σ_1 with respect to the olivine crystal lattice. (010) is preferred as a glide plane for [100] slip over a wider range of orientations of σ_1 than are any of the other (0kℓ) glide planes (Fig.9, Durham, 1975).

Our specimens are behaving very similar to Fig. 9. The a-c orienta-

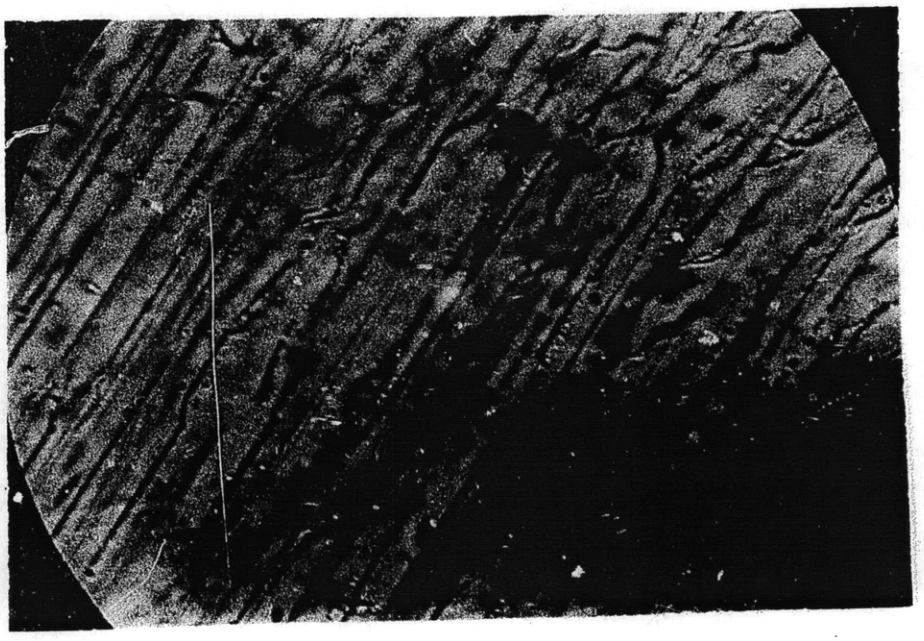

Fig. 10 a-c orientation bubble train, field of view 110μ

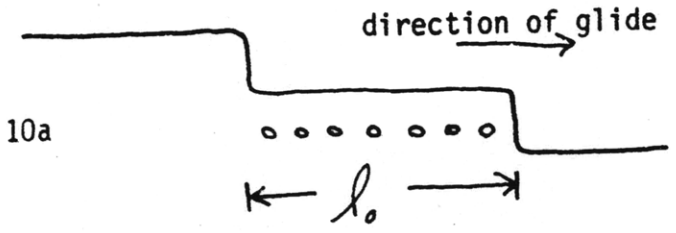

ℓ_o = distance dislocation moved

tions were not exactly 45^0 and therefore fell into the second region of (021)[100], (011)[100] in Fig. 10. A more generalized glide plane of (0kℓ) fits our specimens.

Canon and Sherby (1973) described two classifications of alloys. Class I alloy had n = 3 while Class II had n = 5. Where n = 5, the creep rate was controlled by dislocation climb. For n = 3, the controlling mechanisms was described as a charged cloud being dragged along by the dislocation. Canon and Sherby tentatively suggested that where anion-cation ratios are large, creep is of the form σ^3. The implication is that for dislocations that are strongly charged the glide step is the slowest and therefore rate controlling step. For n = 5, the dislocations may be only weakly charged, and the glide may be rapid so that dislocation climb is rate controlling (Canon and Sherby, 1973). The creep exponent, n = 3, is compatible with a glide limited creep law only if glide follows a 'viscous' law $V_{glide} = \sigma^{-1} f(T)$. This follows from the fact (shown for olivine in Kohlstedt and Goetze, (1974)) that the dislocation density is of the form $\rho \propto \sigma^{-2}$ so that $\dot{\epsilon} = \rho b V_{glide}$ must correspond to only a single power stress dependence of V_{glide}. Alexander and Haasen, 1968, found that the velocity stress exponent for Ge, Si, and InSb is close to one. Takeuchi and Argon (1976), have calculated that $\dot{\epsilon}$ is limited by glide alone for Class I alloys. In our case, olivine certainly is a Class I alloy as described by Canon and Sherby (1973).

Is the creep rate in these olivine single crystals limited by the glide velocity? To test this we attempted to compute Durham's creep data from the formula $\dot{\epsilon} = \rho b V_{glide}$ using the experimental V_{glide} data from Tables 3 and 4 and dislocation densities from the observed relation

TABLE 3

Data for 'a-b' orientations

Specimen	$\sigma_1-\sigma_3$ (kbars)	T (^oC)	ℓ_o* (μ)	t (sec)	V (cm/sec)	ρ (cm^{-2})
7510-1B	2.5	1265	-	1200	-	-
	1.4	1265	30	1200	2.50×10^{-6}	4.64×10^{8}
	1.0	1265	45	1200	3.75×10^{-6}	2.37×10^{8}
	.8	1265	50	1200	4.17×10^{-6}	1.51×10^{8}
	.5	1265	30	1200	2.50×10^{-6}	5.92×10^{7}
	.3	1265	20	1200	1.67×10^{-6}	2.13×10^{7}
7510-2B	1.2	1150	-	-	-	-
	broken during assembly					
7510-3B	1.4	1155	< 3	600	<5 x10^{-7}	4.64×10^{8}
	no apparent motion -- minimum value determined					
7510-4B	2.4	1080	<5	1800	$<2.78\times10^{-7}$	1.36×10^{8}
	no apparent motion -- minimum value determined					
7510-5B	.47	1120	-	1800	-	-
	sample tilted in holder -- stress was not perpendicular to face					
7510-6B	.50	1350	<5	1800	$<2.78\times10^{-7}$	5.92×10^{7}
	no apparent motion -- minimum value determined					
7510-7B	.47	1400	< 5	480	$<1.04\times10^{-6}$	5.23×10^{7}
	no apparent motion -- minimum value determined					

* where ℓ_o is movement of dislocation

TABLE 3 (cont)

Specimen	$\sigma_1-\sigma_3$ (kbars)	T (^oC)	ℓ_o (μ)	t (sec)	V (cm/sec)	ρ (cm^{-2})
7510-8B	2.5	1100	-	9000	-	-
	sample tilted -- stress patterns not easily determined					
7510-9B	1.07	1200	-	1800	-	-
	.85	1200	40	1800	2.22×10^{-6}	1.71×10^{8}
	indents on 'c' face -- no evidence of movement due to indents					
7510-10B	1.5	1200	-	1800	-	-
	heavily indented on 'c' face -- broke during experiment					

TABLE 4

Data for "a-c" orientations

Specimen	$\sigma_1-\sigma_3$ (kbars)	T (^oC)	ℓ. (μ)	t (sec)	V (cm/sec)	ρ (cm^{-2})
7511-1A	1.68	1200	-	1800	-	-
	.84	1200	20	1800	1.11×10^{-6}	1.67×10^{8}
	.50	1200	5	1800	2.78×10^{-7}	5.92×10^{7}
7511-2A	1.0	1350	-	1800	-	-
	sample was broken during assembly					
7511-3A	1.04	1350	-	1800	-	-
	.73	1350	40	1800	2.22×10^{-6}	1.25×10^{8}
	.73	1350	26	1800	1.44×10^{-6}	1.25×10^{8}
	.70	1350	15	1800	8.33×10^{-7}	1.16×10^{8}
	.50	1350	5	1800	2.78×10^{-7}	5.96×10^{7}
	.49	1350	32	1800	1.78×10^{-6}	5.61×10^{7}
	.49	1350	25	1800	1.38×10^{-6}	5.61×10^{7}
	.40	1350	15	1800	8.33×10^{-7}	3.69×10^{7}
	.36	1350	27	1800	1.50×10^{-6}	3.14×10^{7}
7511-4A	2.0	1130	29	1800	1.61×10^{-6}	9.47×10^{8}
	1.7	1130	35	1800	1.94×10^{-6}	7.00×10^{8}
	1.4	1130	5	1800	2.78×10^{-7}	4.64×10^{8}
	1.2	1130	48	1800	2.67×10^{-6}	3.41×10^{8}
	1.2	1130	10	1800	5.56×10^{-7}	3.41×10^{8}
	1.0	1130	26	1800	1.44×10^{-6}	2.37×10^{8}
	1.0	1130	29	1800	1.61×10^{-6}	2.37×10^{8}

TABLE 4 (cont)

Specimen	$\sigma_1-\sigma_3$ (kbars)	T (^oC)	ℓ_o (μ)	t (secs)	V (cm/sec)	ρ (cm^{-2})
7511-4A (cont)	.6	1130	15	1800	8.33×10^{-7}	8.52×10^{7}
	.5	1130	17	1800	9.44×10^{-7}	5.92×10^{7}
7511-5A	.08	1450	<5	1800	$<2.78\times10^{-7}$	1.52×10^{6}
	no apparent motion therefore a minimum value is given					
7511-6A	1.3	1200	-	1800	-	-
	1.2	1200	70	1800	3.89×10^{-6}	3.41×10^{8}
	1.04	1200	60	1800	3.33×10^{-6}	2.56×10^{8}
	1.04	1200	60	1800	3.33×10^{-6}	2.56×10^{8}
	.9	1200	10	1800	5.56×10^{-7}	1.92×10^{8}
	.78	1200	40	1800	2.22×10^{-6}	1.44×10^{8}
	diamond scratches on 'b' face					
7511-7A	2.0	1250	-	1800	-	-
	diamond scratches on 'b' and 'a-c' faces weakened specimen -- broken during experiment					
7511-8A	1.7	1250	-	1800	-	-
	broken during experiment					
7511-9A	1.2	1470	-	100	-	-
	.48	1470	30	100	3.00×10^{-5}	5.45×10^{7}
	.30	1470	25	100	2.50×10^{-5}	2.13×10^{7}
	sample underwent measurable bending plastically					

TABLE 4 (cont)

Specimen	$\sigma_1-\sigma_3$ (kbars)	T (^oC)	ℓ_o (μ)	t (secs)	V (cm/sec)	ρ (cm^{-2})
7511-10A	2.0	1575	>162	10	$>1.62\times10^{-3}$	9.47×10^{8}
	dislocation motion was extremely fast					
7511-11A	1.0	1500	<5	2	$<2.5\times10^{-4}$	2.37×10^{8}
	no apparent motion -- minimum value determined					
7511-12A	2.0	1150	-	3000	-	-
	broken during assembly					
7511-13A	1.0	1400	<5	10	$<2.0\times10^{-5}$	2.37×10^{8}
	no apparent motion -- minimum value determined					
7511-14A	.3	1550	-	1050	-	-
	.25	1550	15	1050	1.43×10^{-6}	2.13×10^{7}
7511-15A	2.0	1150	-	3000	-	-
	broken during experiment					
7511-16A	2.0	1240	<5	300	$<1.67\times10^{-6}$	9.47×10^{8}
	no apparent motion -- minimum value determined					

(Kohlstedt and Goetze, 1974) for steady-state creep.

$$\sigma_1 - \sigma_3 = \alpha \mu b \rho^{.5}$$

$\alpha \sim$ constant $\sim$ 2-3
b = Burgers vector
$\sigma_1 - \sigma_3$ = differential stress

In order to make a comparison with Durham's data stresses have been corrected to a common strain rate of 10^{-5} 1/sec. This was done using n = 4.3 for the a-c orientations and n = 3.6 for the a-b orientations. At higher stresses and lower temperatures there is some ambiguity in Durham's data about the appropriate value of n, for the a-c orientation, values between 5 and 3.6 being compatible with all data. n = 4.3 simply represents a compromise. Stress corrections were generally modest and the data is therefore not sensitive to the choice of n. These corrected stresses are compared with Durham's data in Figs. 11 and 12. Additional data with similar experimental technique by Evans (unpublished) is also shown. The large solid circles are Durham's data and the open circles Phakey et al.

Our conclusion is that within the scatter the strain rates so computed to agree with Durham's data indicating that glide appears to be the limiting step.

Whether the large scatter results from the obvious inaccuracies in the technique or whether the glide velocity itself will show considerable scatter once a better method is used is a question we cannot answer at this stage.

CONCLUSIONS

The strain rate of a-b and a-c oriented single crystals of olivine

is probably glide limited.

TABLE 5

Experimental data for dry olivine single crystals

"a-b" orientation

Specimen	$\sigma_1-\sigma_3$ (kbars)	T (^{o}C)	$\dot{\epsilon}$ (10^{-5}/sec)	$\log_{10}\dot{\epsilon}$	$\sigma_{corrected}$
7510-1B	1.4	1265	5.80	-4.24	.86
	1.0	1265	4.44	-4.35	.66
	.8	1265	3.15	-4.5	.58
	.5	1265	.74	-5.13	.54
	.3	1265	.18	-5.74	.48
7510-3B	1.4	1155	.246	-4.9	1.3
7510-4B	2.4	1086	.18	-5.72	3.8
7510-6B	.5	1350	.082	-6.08	1.0
7510-7B	.47	1400	.272	-5.57	.68
7510-9B	.85	1200	1.90	-4.72	.71

TABLE 6

Experimental data for dry olivine single crystals

"a-c" orientations

Specimen	$\sigma_1-\sigma_3$ (kbars)	T (^{o}C)	$\dot{\varepsilon}$ (10^{-5}/sec)	$\log_{10}\dot{\varepsilon}$	$\sigma_{corrected}$
7511-1A	.84	1200	.93	-5.03	.85
	.5	1200	.08	-6.10	.9
7511-3A	.73	1350	1.39	-4.86	.66
	.73	1350	.90	-5.05	.75
	.70	1350	.48	-5.32	.83
	.5	1350	.08	-6.10	.90
	.49	1350	.50	-5.30	.58
	.49	1350	.39	-5.41	.61
	.4	1350	.15	-5.82	.62
	.36	1350	.24	-5.62	.50
7511-4A	2.0	1130	7.62	-4.12	1.25
	1.72	1130	6.79	-4.17	1.10
	1.4	1130	.64	-5.19	1.55
	1.2	1130	4.55	-4.34	.84
	1.2	1130	.95	-5.02	1.21
	1.0	1130	1.91	-4.72	.86
	1.0	1130	1.71	-4.77	.88
	.6	1130	.35	-5.46	.77
	.5	1130	.28	-5.55	.67
7511-5A	.08	1450	.002	-7.68	.339

TABLE 6 (cont)

Specimen	$\sigma_1-\sigma_3$ (kbars)	T (^oC)	$\dot{\varepsilon}$ (10^{-5}/sec)	$\log_{10}\dot{\varepsilon}$	$\sigma_{corrected}$
7511-6A	1.2	1200	6.63	-4.18	.77
	1.04	1200	4.26	-4.37	.74
	1.04	1200	4.26	-4.37	.74
	.9	1200	.53	-5.28	1.04
	.78	1200	1.60	-4.80	.70
7511-9A	.48	1470	8.18	-4.09	.29
	.3	1470	2.66	-4.58	.24
7511-10A	2.0	1575	7668.	-1.12	.25
7511-11A	1.0	1500	295.	-2.53	.27
7511-13A	1.0	1400	23.6	-3.63	.48
7511-14A	.3	1550	.15	-5.82	.47
7511-16A	2.0	1240	7.90	-4.10	1.24

Figures 11 and 12

Large circles represent experimentally measured creep data. Triangles, points and bars represent stresses computed from dislocation glide data as described in the text. Points with arrows indicate upper or lower limits.

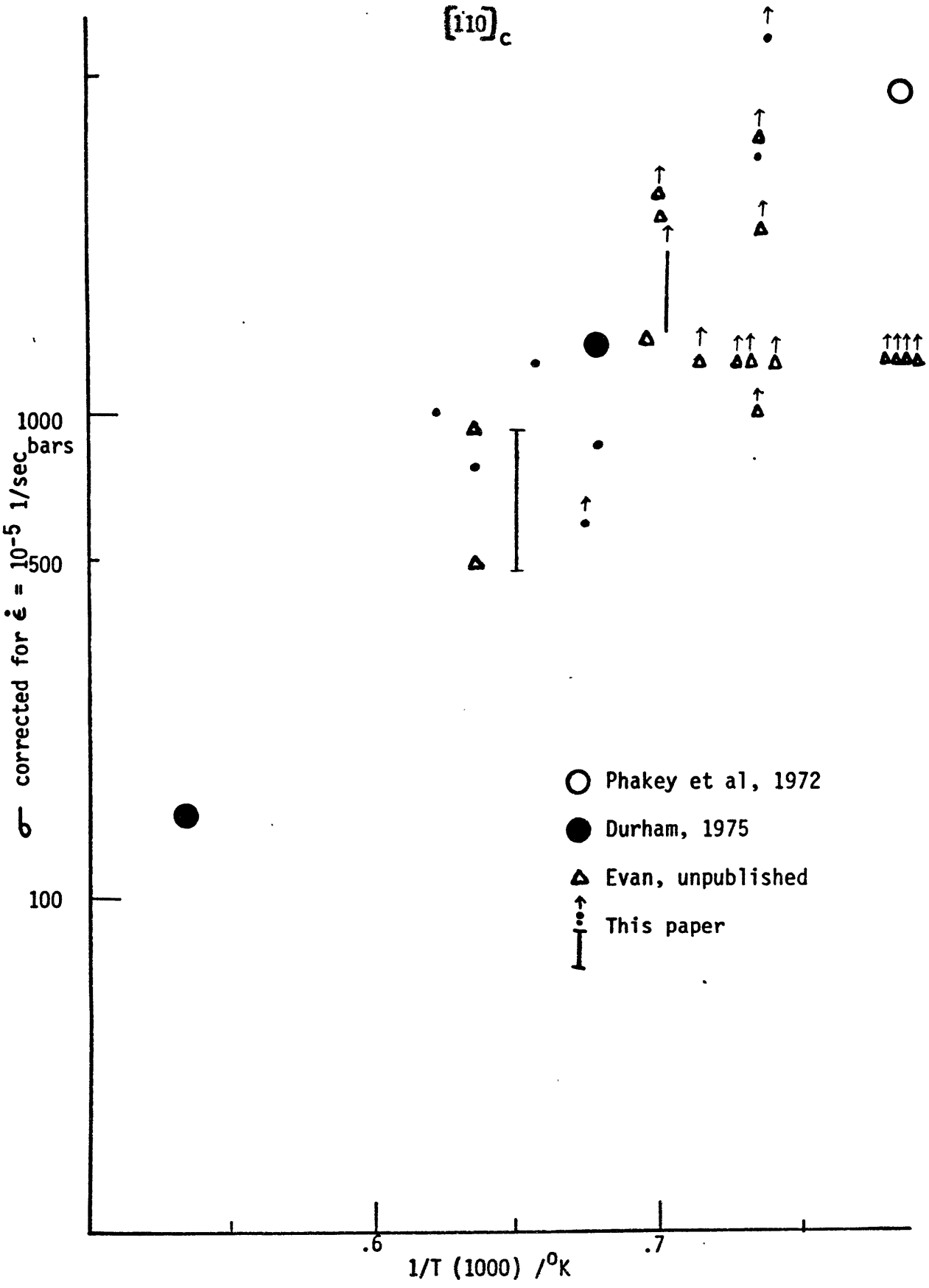
[110]c
1000
500
100
σ corrected for ε̇ = 10-5 1/sec bars
.6
.7
1/T (1000) /°K
Phakey et al, 1972
Durham, 1975
Evan, unpublished
This paper

Fig. 11

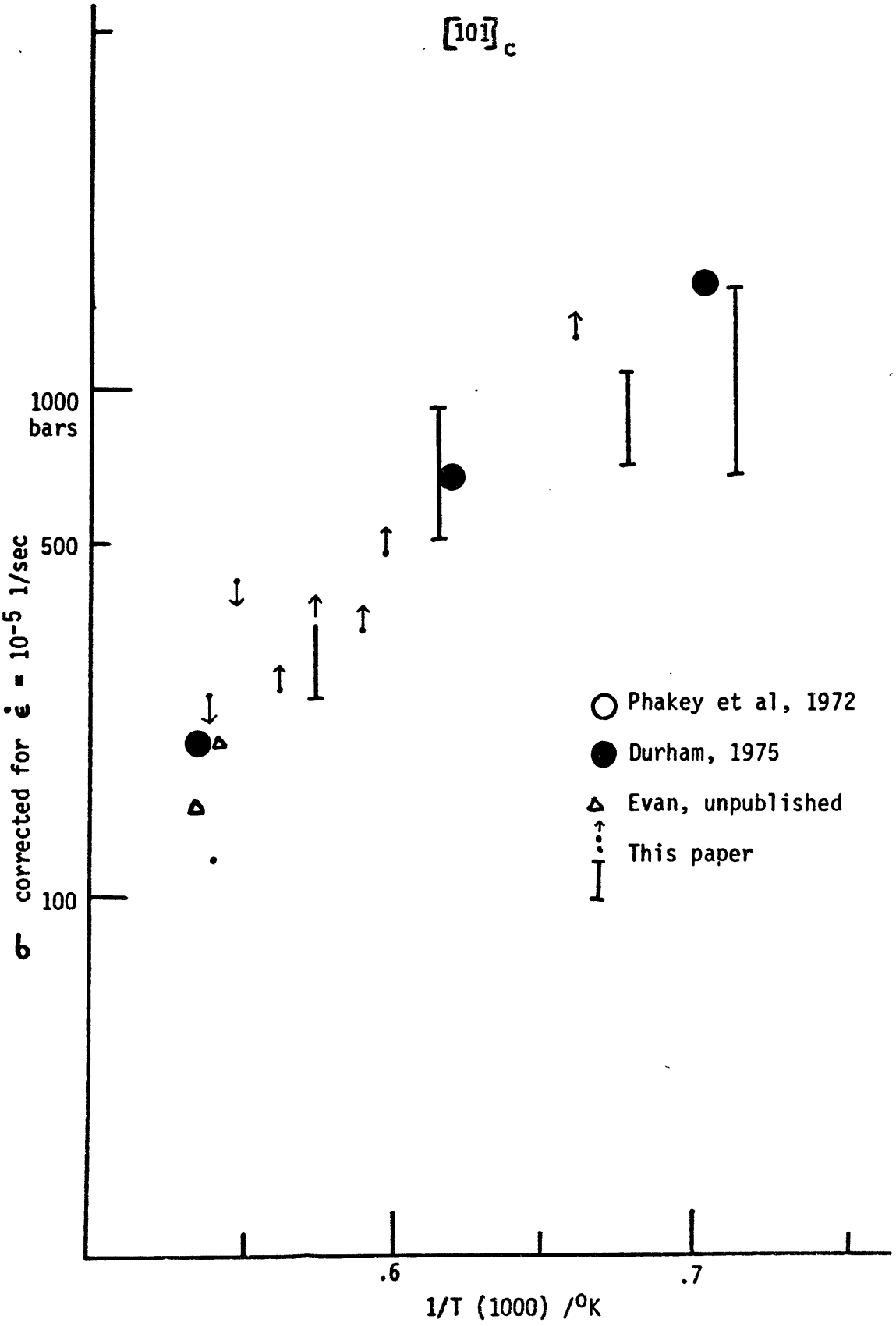
[101]c
1000 bars
500
100
σ corrected for ε̇ = 10-5 1/sec
Phakey et al, 1972
Durham, 1975
Evan, unpublished
This paper
.6
.7
1/T (1000) /°K

Fig.12

BIBLIOGRAPHY

Alexander, H. and P. Haasen, Dislocations and plastic flow in the diamond structure, in Solid State Physics, 22, p.27, edited by F. Seitz, D. Turnbull, and H. Ehrenreich, Academic Press, New York, 1968.

Canon, W. and O. Sherby, Third power stress dependence in creep of polycrystalline nonmetals, Journal of American Ceramic Society, 157, 1973.

Chaudhuri, A. R., J. R. Patel and L. G. Rubin, Velocities and densities of dislocations in Germanium and other semiconductor crystals, Journal of Applied Physics, 33, p.2736, 1962.

Cottrell, A. H., Dislocations and Plastic Flow in Crystals, Clarendon Press, Oxford, 1953.

Durham, W. B., Plastic Flow of Single-Crystal Olivine, PhD., M.I.T., 1975.

Evans, B., Unpublished data, 1975.

Freidel, J., Dislocations, Addison-Wesley, Reading, Mass., 1964.

Goetze, C. and D. L. Kohlstedt, Laboratory study of dislocation climb and diffusion in olivine, Journal of Geophysical Research, 78, p. 5961, 1973.

Hull, D., Introduction to Dislocations, Pergamon Press, New York, 1965.

Johnston, W. G. and J. J. Gilman, Dislocation velocities, dislocation densities, and plastic flow in Lithium Fluoride crystals, Journal of Applied Physics, 30, p.129, 1959.

Kelly, A. and G. W. Groves, Crystallography and Crystal Defects, Addison-Wesley Publishing Co., Reading, Massachusetts, 1970.

Kohlstedt, D. L. and C. Goetze, Low-stress high-temperature creep in olivine single crystals, Journal of Geophysical Research, 79, p.2045, 1974.

Kohlstedt, D. L., C. Goetze, and W. B. Durham, Experimental deformation of single crystal olivine with application to flow in the mantle, in Petrophysics: The Physics and Chemistry of Minerals and Rocks, edited by S. K. Runcorn, John Wiley and Sons, Ltd., London, in press, 1975a.

Nitsan, U., The stability field of olivine with respect to oxidation and reduction, Journal of Geophysical Research, 79, p.706, 1974.

Phakey, P.,G. Dollinger, and J. Christie, Transmission electron microscopy of experimentally deformed olivine crystal, in Flow and Fracture of Rocks Geophysical Monograph Series, vol. 16, edited by H. C. Heard, I. Y. Borg, N. L. Carter, C. B. Raleigh, p. 117, A.G.U., Washington, D. C., 1972.

Prekel, H. L. and H. Conrad, Dislocation velocity and deformation dynamics in Molybdenum..

Raleigh, C. B., Glide mechanisms in experimentally deformed minerals, Science, 150, p.739, 1965.

Raleigh, C. B., Mechanisms of plastic deformation of olivine, Journal of Geophysical Research, 73, p.5391, 1968.

Singh, R. N. and R. L. Coble, Dynamic dislocation behaviour in "pure" magnesium oxide single crystals, Journal of Applied Physics, 45, p.981, 1974.

Takeuchi, S. and A. Argon, Steady state creep of alloys due to viscous motion of dislocations, in press, 1976.

Takeuchi, S. and A. Argon, A review paper--Steady state Andrade creep of single-phase crystals at high-temperature, unpublished paper, 1976.

Timoschenko and Goodier, Theory of Elasticity, Engineering Societies Monographs, 2nd edition, McGraw-Hill Co., 1951.

Weertman, J., Dislocation climb theory of steady-state creep, Transactions of American Society Metals, 61, p.681, 1968.

Young, III, C., Dislocations in the deformation of olivine, American Jornal of Science, 267, p.841, 1969.